

Magneto-optical effects with cold lithium atoms

S Franke-Arnold¹, M Arndt² and A Zeilinger²

¹ University of Strathclyde, Department of Physics and Applied Physics, 107 Rottenrow East, Glasgow G4 0NG, UK

² Universität Wien, Institut für Experimentalphysik, Boltzmannngasse 5, A-1090 Wien, Austria

Received 17 May 2001

Abstract

We report measurements of magneto-rotational effects in the coherent forward scattering of light on an ensemble of cold ⁷Li atoms. The effect of the cold atomic cloud on the polarization state of a probe beam is studied for magnetic fields in the Faraday and Voigt configurations. Magneto-optical effects with cold atoms have the potential to be highly sensitive tools for the spatially and temporally resolved detection of either small atomic ensembles or small magnetic fields.

1. Introduction

Ever since Faraday discovered that the polarization state of light is affected by a magnetic field in the medium that it traverses [1], this and other magneto-optical effects have been intensely studied and various other applications have been found.

The interaction strength of light with matter depends strongly on the detuning between the probe light and the resonance line in the material as well as on the optical linewidth of the atomic sample. The same parameters also determine the strength of magneto-rotational effects. In the case of liquids or solids—materials conventionally used for technological implementations of magneto-rotation—the employed light sources are usually far detuned from all resonance lines. The detuning can amount to several hundred nanometres and the linewidth to some tens of nanometres, so that the resulting magneto-optical effects in these applications are comparatively small. In order to achieve a significant polarization rotation one requires typically about 10^{23} scatterers and magnetic fields of the order of 1000 Gauss.

Dilute atomic ensembles, however, exhibit resonance lines that can easily be accessed by available lasers. This allows one to exploit the strong resonant enhancement of magneto-optical effects, a fact discovered by Macaluso and Corbino at the turn of the 19th century [2].

Already, room temperature gas cell experiments using alkaline atoms provide a tremendous improvement in magnetic sensitivity [3]. The linewidth is then typically four orders of magnitude smaller than in solid samples, limited only by collisions and Doppler broadening. In vapour cell experiments the perturbation of the atoms can be reduced with the help of wall coatings or buffer gases and magnetic coherence times of the order of one second have

been achieved [4]. Such arrangements have successfully been exploited for high precision magnetometry and for fundamental tests of symmetry violations in atoms.¹

Laser cooled atoms are interesting candidates for magneto-optical experiments since they exhibit Doppler and collision free optical and magnetic transitions and have the potential to be trapped over long times. Since the advent of laser cooling techniques [7] it has become routine to cool atoms to velocities of a few centimetres per second and to trap them in far-detuned optical fields. Consequently, Doppler broadening and collisions can almost be completely neglected. In a recent experiment on a sample of cold dense Rb atoms, a Verdet constant of about $170 \text{ rad T}^{-1} \text{ m}^{-1}$ and a maximal polarization rotation of $5/6\pi$ rad was achieved [8]. Even narrower effective linewidths resulting in higher magnetic sensitivity are to be expected in Bose–Einstein condensates. Lifetimes of as high as 20 s have been demonstrated [9] with an effective linewidth of $\approx 2 \text{ kHz}$ [10]. Cold atom samples thus provide very sensitive and well-localized probes for the study of small external magnetic fields. Alternatively, magneto-rotational effects can be used as precise tools for the investigation of the atomic properties of the sample.

The sensitivity to magnetic fields can be greatly enhanced by employing techniques which monitor the atomic orientation [11] and alignment [12] or exploit the magnetic ground state coherences.² However, the linear Faraday and Voigt rotations of light interacting with cold atoms already provide a simple, robust and rather sensitive method for magnetometry with a high spatial and temporal resolution. It is noteworthy that these linear effects are important enough to show up even when the experiment is not particularly designed to measure them and may therefore be of relevance in certain configurations of time dependent atom-interferometry [15], coherent forward scattering in measurements of the collective atomic spin [16], coherent back scattering [17] or the non-destructive polarization imaging of Bose–Einstein condensates [18].

In our present experiment, we demonstrate magneto-optical effects using an ensemble of ^7Li atoms that are trapped and cooled to a few $100 \mu\text{K}$. Subsequently they are probed in an external magnetic field by linearly polarized light. We have investigated the homogeneous longitudinal (Faraday) and transverse (Voigt) geometry. It might be interesting to note that the cold atomic ensemble acts as a point-like magnetometer with a dimension given by the diameter of the atomic cloud.

2. Experimental set-up and results

For the measurements of the Faraday effect, a weak linearly polarized probe light beam traverses the cold atomic cloud in the direction parallel to an external magnetic field as depicted in figure 1(a). The polarization state after the interaction is then analysed by means of a balanced detector, composed of a polarizing beam splitter (PBS), at an angle of 45° with respect to the incoming probe beam polarization and two fast Si-photodiodes. Their difference signal is a measure of the polarization rotation whilst their sum is used for normalization purposes.

In the Faraday configuration the magnetic field direction is the natural choice for the quantization axis. For small magnetic fields, LS coupling can be assumed and the Zeeman levels within a hyperfine state are shifted by $\Delta E = -\mu_B m_F g_F B$. Here μ_B denotes the Bohr

¹ In order to reduce the collisional or Doppler broadening, atomic beams have successfully been used together with a transverse excitation of the atoms. The price to pay is a limitation of any measurement by the relatively short time of flight even though one can greatly improve on this using pump–probe techniques in a Ramsey configuration, see e.g. [5]. For a recent review on PNC experiments with atoms see [6].

² The implementation of electromagnetically induced transparency (EIT) in cold atoms has been demonstrated by [13]. Systems of this kind seem extremely promising for high-sensitivity magnetometry, see e.g. [14].

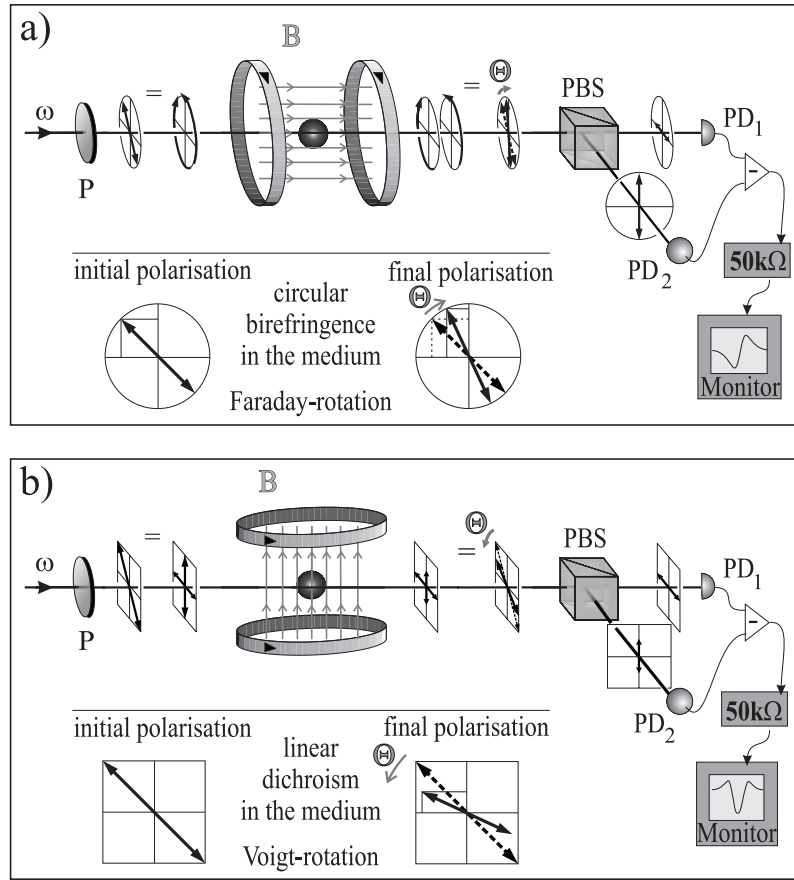


Figure 1. Sketch of the experimental set-up for measuring the Faraday (a) and Voigt effects (b).

magneton, m_F the magnetic quantum number, g_F the Landé factor and B the magnetic field amplitude. The resonance frequencies for left and right circularly polarized light driving these transitions are therefore also shifted by the applied magnetic field as indicated in the level scheme in figure 2. This gives rise to a variation of the corresponding refractive indices, $n_+(v)$ and $n_-(v)$ [19]. The circular decomposition components of linearly polarized light will then experience different refractive indices and acquire different phase shifts while propagating through a medium of length L . This magnetically induced circular birefringence thus results in a polarization rotation per unit length of $\frac{2\pi}{\lambda} \text{Re}(n_- - n_+)$. The overall rotation of polarization is obtained by integrating this quantity over the path of the light beam through the trapped atoms,

$$\Theta_{\text{Faraday}} = \frac{2\pi}{\lambda} \int_{-\infty}^{\infty} dz \text{Re}(n_- - n_+). \quad (1)$$

We note that the rotation angle, as well as the refractive index, depends to first order linearly on the number of interacting atoms of the sample.

For measurements of the Voigt effect, the external magnetic field is rotated by 90° with respect to the Faraday case and thus is perpendicular to the k -vector of the incoming light beam. The rest of the set-up remains identical and is sketched in figure 1(b).

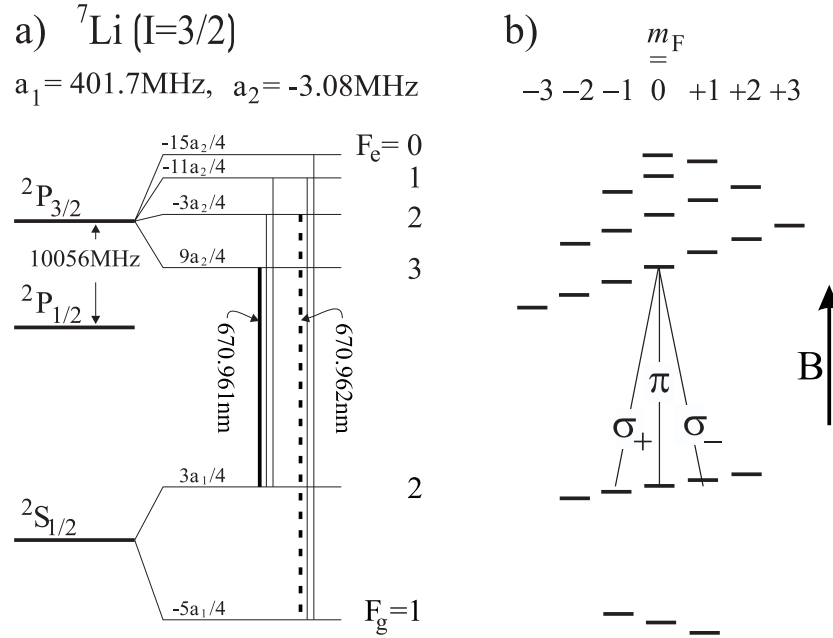


Figure 2. The relevant energy level scheme of lithium. The trapping and re-pumping transitions are indicated by the full and dashed lines, respectively (a). The Zeeman levels split in a magnetic field, so that the resonance frequencies for σ_{\pm} light are shifted compared to that for π light (b).

The prevailing effect in this configuration is the linear dichroism induced by the external magnetic field. Its strength depends on the angle α between the magnetic field and the incident polarization axis as defined by the polarizer P, with a maximum effect at 45° . Again this may be understood from the Zeeman shift of the atomic levels in the magnetic field. If the magnetic field is taken as the common quantization axis, the incoming linear polarization can be split up into components parallel and perpendicular to the magnetic field, as indicated in figure 1(b). The absorption coefficient of the parallel component is, to first order, unaffected by the magnetic field. The perpendicular light component, however, may be thought of as a superposition of right and left circularly polarized light with respect to the quantization axis in the direction of the magnetic field. Hence, the absorption depends on the magnetic field and the overall polarization is rotated by the angle

$$\Theta_{\text{Voigt}} = \frac{2\pi}{\lambda} \sin(2\alpha) \int_{-\infty}^{\infty} dz \text{Im}(n_{\parallel} - n_{\perp}). \quad (2)$$

In the experiment the medium was provided by ${}^7\text{Li}$ atoms that were previously cooled and trapped in a magneto-optical trap. The atoms were loaded from a thermal beam in a vacuum chamber at a base pressure of a few 10^{-9} Torr. All light beams needed for trapping, cooling, re-pumping, slowing and probing were derived from the same dye laser using acousto-optic (AOM) and electro-optic (EOM) modulators. For trapping, the closed transition ${}^2\text{S}_{1/2}$, $F = 2$, $m_F = 2 \rightarrow {}^2\text{P}_{3/2}$, $F = 3$, $m_F = 3$ at 670.962 nm was used, indicated in figure 2. We note that throughout this paper every detuning is given compared to this transition. A simple slower beam, red detuned by 90 MHz, increased the number of atoms in the trap by a factor of 5. As the hyperfine levels of the excited state are separated by at most ≈ 18 MHz, atoms can be lost from the trapping cycle by excitation to another hyperfine level

followed by a decay to the lower ground state $^2S_{1/2}, F = 1$. These atoms were re-pumped into the trapping cycle on the transition $^2S_{1/2}, F = 1 \rightarrow ^2P_{3/2}, F = 2$. An EOM modulated at 803.5 MHz generated the required light as the blue sideband of the trapping light. A total intensity of ≈ 200 mW was used for the MOT beams. Both trapping and probe light could be switched independently in about 20 ns by the AOMs. The density of the trapped atoms was measured by absorption and fluorescence measurements to be about $2 \times 10^{10} \text{ cm}^{-3}$ with a temperature of $800 \pm 200 \mu\text{K}$. The quadrupole magnetic field of the MOT had a typical gradient of 12 G cm^{-1} in the axial direction. The homogeneous Faraday and Voigt fields could be set to values in the range of 0.1–100 G. All magnetic field coils were positioned inside the vacuum chamber in order to reduce induced currents after switching. The typical rise and decay times of the magnetic fields were $40 \mu\text{s}$ and $10 \mu\text{s}$, respectively.

The experiment was run with successive phases of trapping in the MOT (2s), cooling in optical molasses (30 ms), evolution in the homogeneous field (300 μs in order to exclude any switching effects during probing) and probing the cold atomic ensemble (1.7 ms). A homogeneous probe beam intensity profile was established by using only the innermost part of the Gaussian laser beam. During probing the EOM could be switched off so that only the transition from $^2S_{1/2}, F = 2$ to the excited state was driven. The polarization rotation of the probe beam was measured with the balanced measurement scheme mentioned above. It uses the fact that a rotation of the polarization direction produces an asymmetry in the photo-currents recorded by the two photodiodes PD₁ and PD₂, as indicated in figure 1. The difference, D , of these signals was monitored as a function of time on an oscilloscope and averaged over 150 samples. Additionally, the sum S of the two photodiodes was recorded for normalization.³ The angle of rotation is then given by

$$\Theta_{\text{Faraday, Voigt}} = \frac{1}{2} \arcsin\left(\frac{D}{S}\right) \approx \frac{D}{2S}. \quad (3)$$

The Faraday measurements were performed with a probe beam diameter of 2.5 mm. The chosen probe beam intensity of $50 \mu\text{W}$ corresponds then to about 20% of the saturation intensity $I_{\text{sat}} = 25.33 \text{ W m}^{-2}$. The homogeneous magnetic field was preset by adjusting the current through the Helmholtz coils. For every chosen magnetic field the polarization rotation was then recorded as a function of time after switching on the probe beam. Figure 3(a) shows a selection of such curves. The rotation is maximal during the first few microseconds and decays exponentially with a relaxation time that depends on the magnetic field. This decay arises from the proportionality of the rotation angle to the number of interacting atoms. In our case the strongest relaxation process is the decay into the lower hyperfine state of the ground level $|F = 1\rangle_{\text{g}}$ via an excitation from $|F = 2\rangle_{\text{g}} \rightarrow |F = 2\rangle_{\text{e}}$ followed by spontaneous decay. For near-resonant light the effective detuning depends strongly on the Zeeman-detuning which has a contribution of $\approx \Gamma/6$ per Gauss. In a high magnetic field an excitation therefore becomes less likely and the atom remains longer in the probed ground state $|F = 2\rangle_{\text{g}}$ which results in a slower decay of the Faraday rotation.

From the time-dependent rotation curves at various magnetic fields in figure 3(a) we extracted fig 3(b) which shows the Faraday rotation as a function of the magnetic field at different probing times. The qualitative shape of the Faraday rotation can be understood by considering the dispersion curves of σ_+ and σ_- light according to equation (1). Applying a magnetic field corresponds to shifting these dispersion curves with respect to each other and

³ The difference signal is given by $D = E_0^2 \sinh(2\psi_{\text{Faraday}}z)$, where E_0 is the amplitude of the probe light field. The sum signal in fact measures the angle of ellipticity, ψ_{Faraday} , of the probe beam which results from the different absorption of the right and the left circularly polarized components in the magnetic field, $S = E_0^2 \cosh(2\psi_{\text{Faraday}}z)$. For small angles of ellipticity, as in this work, \cosh can be approximated to 1 and the sum signal can be used for normalization.

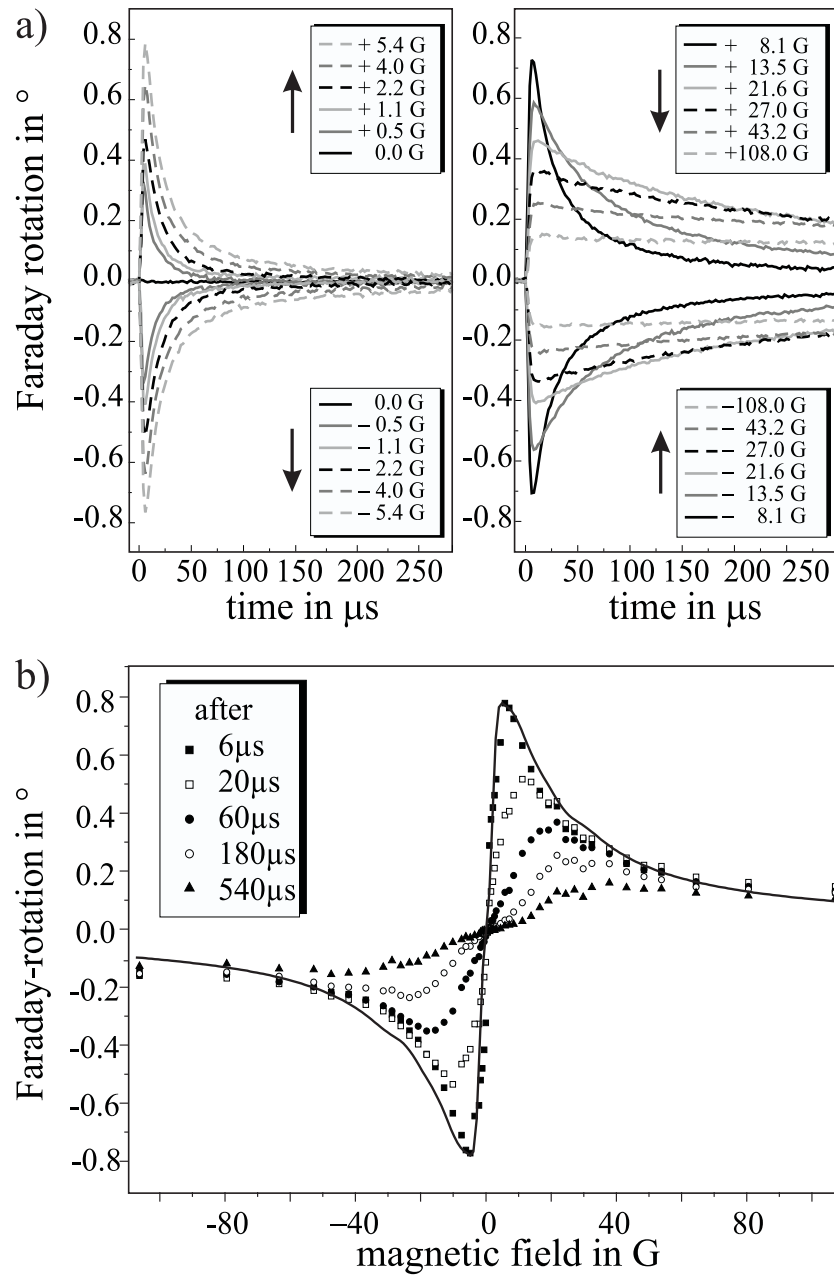


Figure 3. (a) Selection of the primary time resolved measurements from which the magnetic field dependence shown in figure 4 was derived. The experiments were performed with near-resonant light at 20% of the saturation intensity. (b) Measurement and simulation (full curve) of the Faraday effect as a function of the magnetic field. The different curves show the Faraday effect at different times after switching on the probe beam.

the measurement determines the difference of dispersion at the probe beam frequency. As the dispersion curves are centred around the atomic resonance frequency, the Faraday signal

shows distinct features near resonance and the probe beam frequency was chosen accordingly. A large positive or negative magnetic field effectively corresponds to a comparison of the dispersion of far red with far blue detuned light and thus results in small signals. For magnetic fields of a few Gauss, however, the Larmor frequency is of the order of the atomic linewidth and the Faraday signal becomes maximal when the effective detuning corresponds to $\Gamma/2$. For smaller magnetic fields the dispersion curves overlap more and more until the polarization signal vanishes completely at $B = 0$. We note that there is an apparent shift of the maximal angle of rotation towards higher magnetic fields as the probe time increases (cf figure 3(b)). This is consistent with the assumption that atoms are lost for the interaction with the probe beam by hyperfine pumping. This loss mechanism becomes less effective with increasing magnetic fields due to Zeeman detuning.

The data were recorded between $6 \mu\text{s}$ and $540 \mu\text{s}$ after the probe beam was switched on, with the trap switched off $300 \mu\text{s}$ before that. The measured initial polarization rotation (squares in figure 3(b)) coincides strongly, both in shape and magnitude, with the numerical simulation (full curve).⁴ For the calculation, a detuning of $+2.5 \text{ MHz}$ and an atomic density of $n = 2 \times 10^8 \text{ cm}^{-3}$ in the interaction region were assumed. The loss in the effective atomic density with respect to its value in the trap is partly caused by the diffusion of the atomic cloud during the delay between trapping and probing. However, a major impact is also the optical pumping of population into the lower hyperfine level during the measurement. For lithium this is unavoidable (without a perturbing supplementary re-pumping beam) due to the particularly dense hyperfine structure of the excited state.

The strength of the Faraday rotation is commonly expressed by the Verdet constant, which in our case amounts to $V = 2.5 \times 10^4 \text{ rad T}^{-1} \text{ m}^{-1}$ for magnetic fields under 5 G. Due to the inhomogeneous density distribution of the atomic cloud, V is in reality not constant throughout the atomic ensemble. Instead we give an average Verdet constant for an estimated diameter of the expanding atomic cloud at the time of the measurement of about 4 mm. Considering an atomic density of $n = 2 \times 10^8 \text{ cm}^{-3}$ and a probe beam diameter of 2.5 mm this corresponds to a polarization rotation of $2.6 \times 10^{-5} \text{ rad T}^{-1}$ per atom.⁵

In a similar experiment the Voigt effect, i.e. the influence of a perpendicular magnetic field on the polarization state of a probe beam, was determined. The magnetic field dependence is depicted in figure 4. The polarization rotation of the Voigt effect arises from the different absorption of the light components parallel and orthogonal to the magnetic field as noted in equation (2). While the parallel component is not influenced by the magnetic field, the absorption curve of the orthogonal component consists of a superposition of right- and left-circular light contributions with maxima shifted by the positive and negative Larmor frequency. Without a magnetic field, both absorption curves obviously overlap and the polarization is not rotated. If the magnetic field magnitude rises, one of the maxima of the orthogonal absorption curve gets into resonance with the detuned light which results in an effective rotation of the total polarization. For a further rise the absorption of the orthogonal light component vanishes again and the signal decreases. The magnetic field dependence can therefore be described as 'M'-shaped. We note that the detuning due to the magnetic field for the excited state deviates from the linear Zeeman shift for fields over a few Gauss as LS coupling can no longer be

⁴ Expressions for the frequency dependence of the refractive index and electric susceptibility can be found in [19]. A more realistic theory also has to take into account the existence of the hyperfine and Zeeman manifolds as well as optical pumping between them. This has been included in the numerical simulations of the experimental curves shown in this paper. The theory is, however, restricted to the assumption of LS coupling.

⁵ Magneto-rotation results from coherent scattering processes. We therefore consider the transverse laser area times the longitudinal extension of the atomic cloud as the relevant interaction volume. Each atom contributes to the rotation by the product of the Verdet constant with the length of the interaction region divided by the number of atoms in the interaction volume.

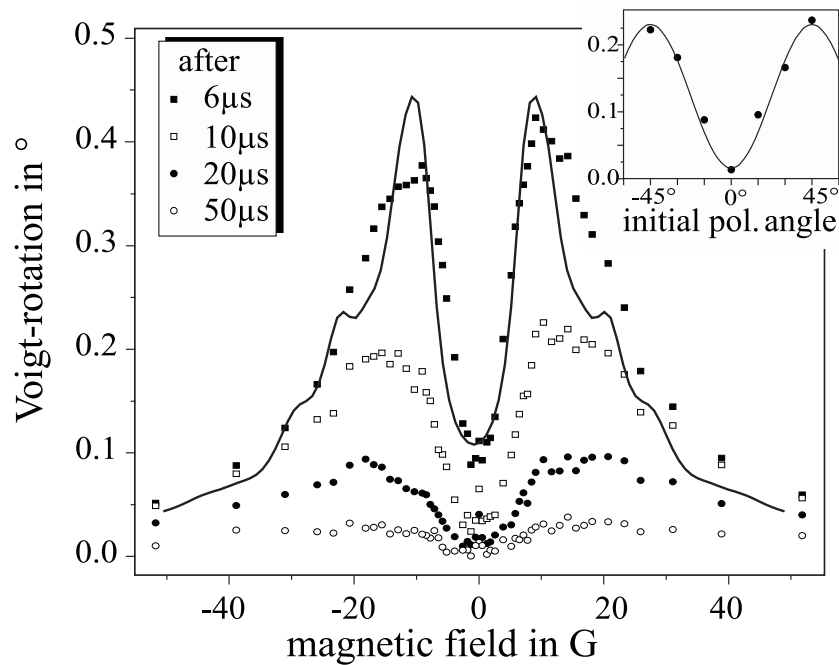


Figure 4. Measurement and simulation of the Voigt effect as a function of the magnetic field. Inset: the Voigt effect varies sinusoidally as a function of the angle between the incident polarization and the magnetic field direction. The rotation is maximal for $\pm 45^\circ$ and vanishes for a polarization parallel or perpendicular to the magnetic field.

assumed, and a simple simulation becomes in principle incorrect. However, the relatively good agreement with the experimental data may justify the neglect of the variation of the momentum coupling with increasing magnetic field. The measurements for figure 4 were performed at a probe detuning of -10 MHz and at 15% of the saturation intensity. At this detuning, 8% of the light is absorbed when no magnetic field is applied. The magnetic field dependence of the Voigt effect was recorded at an initial polarization direction of 45° to the external magnetic field in order to maximize the Voigt effect. This is complemented by the inset of figure 4 which shows the sinusoidal behaviour of the rotation angle for varying initial polarization directions as given by equation (2). This measurement was performed at a constant magnetic field of 12.6 G. Note, that the Voigt effect, arising from absorption, is more sensitive to decay by re-pump processes than the dispersive Faraday effect and accordingly the rotation angle vanishes faster in time. Again, as in the case of the Faraday effect the apparent shift of the rotation maxima towards higher fields with increasing probe time is consistent with the assumed field dependent loss mechanisms.

3. Conclusions

We have experimentally demonstrated the influence of magneto-optical effects in the interaction of a probe laser with a small and cold atomic cloud in a homogeneous magnetic field. Cold atoms exhibit a narrow excitation line given by their natural linewidth, which is one of the reasons for a comparatively strong resonant enhancement of the well-known Faraday and Voigt effects. Magneto-rotation is obviously important in all experiments studying

coherent scattering of light in dilute atomic samples exposed to magnetic fields, for example the quadrupole fields of magnetic or magneto-optical traps. Whilst the integrated Faraday and Voigt effects vanish due to the symmetry of a centrally probed quadrupole field, one can expect a measurable distortion of the polarization field across the laser beam passing through trapped atoms. In some atom interferometry experiments relying on Bragg scattering of light [15], magneto-rotation signals can give rise to unexpected light contributions in otherwise polarization forbidden output-channels of the optical set-up. On the other hand, magneto-optical rotation may be employed for measurements of the atomic density or spin distribution with high spatial and temporal resolution. At the expense of a reduced detection efficiency one can work off-resonance and take advantage of the dispersive magneto-optical effects in order to image polarized cold atomic clouds non-destructively. In particular well localized condensates in traps with strong offset fields [18] are detectable by this method.

Although our present set-up is not competitive in terms of field sensitivity when compared to optimized designs [12–14] we want to stress that dilute cold atomic ensembles offer a high potential for magnetometry when they are combined with a long storage time in non-magnetic, i.e. optical, traps. In particular, we have measured a polarization rotation caused by the Faraday effect of the order of 10^{-5} rad T⁻¹ per atom. This encourages the possibility to perform point-like magnetometric measurements on samples of very few atoms with high spatial and temporal resolution.

Acknowledgments

This work was supported by the FWF under the programme S6504.

References

- [1] Faraday M 1855 *Experimental Research* vol 111 2164
- [2] Macaluso D and Corbino O M 1898 *Nuovo Cimento* **8** 257
- [3] Chen X, Telegdi V L and Weis A 1990 *Opt. Commun.* **74** 301
- [4] Bouchiat M A and Brossel J 1966 *Phys. Rev.* **147** 41
- [5] Budker D, Kimball D F, Rochester S M and Yashchuk V V 2000 *Phys. Rev. Lett.* **85** 2088
- [6] Bouchiat M A and Bouchiat C 1997 *Rep. Prog. Phys.* **60** 1351
- [7] Phillips W D, Gould P L and Lett P D 1988 *Science* **239** 877–83
Cohen-Tannoudji C N and Phillips W D 1990 *Phys. Today* **43** (10) 33–40
Chu S 1991 *Science* **253** 861–6
- [8] Labeyrie G, Miniatura C and Kaiser R 2001 *Phys. Rev. A* to be published
- [9] Mewes M-O *et al* 1996 *Phys. Rev. Lett.* **77** 416
- [10] Stenger J *et al* 1999 *Phys. Rev. Lett.* **82** 4569
- [11] Kastler A 1973 *Nucl. Instrum. Methods* **110** 259
Cohen-Tannoudji C, Dupont-Roc J, Haroche S and Laloe F 1969 *Phys. Rev. Lett.* **22** 758
- [12] Weis A, Wurster J and Kanorsky S I 1993 *J. Opt. Soc. Am. B* **10** 716
Kanorsky S I, Weis A, Wurster J and Hänsch T W 1993 *Phys. Rev. A* **47** 1220
Kanorsky S I, Weis A and Skalla J 1995 *Appl. Phys. B* **60** S165
Budker D, Yashchuk V and Zolotarev M 1998 *Phys. Rev. Lett.* **81** 5788
Drake K H, Lange W and Mlynek J 1988 *Opt. Commun.* **66** 315
- [13] Hau L, Harris S E, Dutton Z and Behroozi C H 1999 *Nature* **397** 594
- [14] Scully M O and Fleischhauer M 1992 *Phys. Rev. Lett.* **69** 1360
Fleischhauer M and Scully M O 1994 *Phys. Rev. A* **49** 1973
Nagel A *et al* 1998 *Europhys. Lett.* **44** 31
- [15] Nic Chormaic S, Franke S, Schmiedmayer J and Zeilinger A 1996 *Acta Phys. Slov.* **46** 463
Kumarakrishnan A, Cahn S B, Shim U and Sleator T 1998 *Phys. Rev. A* **58** R3387
- [16] Soerensen J L, Hald J and Polzik E S 1998 *Opt. Lett.* **23** 1
Kuzmich A *et al* 1999 *Phys. Rev. A* **60** 2346

- [17] Labeyrie G *et al* 1999 *Phys. Rev. Lett.* **83** 5266
- [18] Bradley C C, Sackett C A and Hulet R G 1998 *Phys. Rev. Lett.* **78** 985
- [19] Castera J P 1994 *Encyclopedia of Applied Physics* **9** 157